Inorg. Chem. **1985**, *24*, 4209–4213 **4209**

Notes

Contribution from AT&T Bell Laboratories,
Murray Hill, New Jersey 07974

Generalization of the Topological Electron Counting Rules

Boon K. Teo

Received December 17, 1984

Recently we developed a topological electron counting (TEC) rule for three-dimensional (3-D) polyhedral transition metal clusters.[1] This approach is based on Euler's theorem for polyhedra and the EAN rule for transition metals. Each polyhedron is characterized by a parameter X, which can be determined readily and consistently by a set of simple rules. This theory has been applied to a variety of metal cluster systems.[1b]

In this paper we wish to (1) generalize the TEC theory to include one-dimensional (1-D) and two-dimensional (2-D) clusters as well as clusters containing main-group and/or transition-metal elements and (2) compare the TEC approach with the SEP rule, thereby providing an alternative way of calculating the number of skeletal electron pairs. The relationship of the TEC approach and the polyhedral skeletal electron pair theory (PSEPT) has recently been discussed by Mingos[2] and Teo[3] independently.

The topological electron counting theory[1a] can be extended to include 1-D and 2-D clusters and clusters containing main-group and transition-metal atoms. We shall asume that each main-group atom, with four orbitals, tends to conform to the octet rule and each transition-metal atom, with nine orbitals, tends to attain the 18-electron rule. For a cluster containing V_n main-group atoms and V_m transition-metal atoms at the V vertices ($V = V_n + V_m$), eq 5 of ref 1a becomes

$$T = N/2 = 4V_n + 9V_m - E + X \tag{1a}$$

$$= 3V_n + 8V_m - F + \epsilon + X \tag{1b}$$

where T is the number of topological electron pairs, F is the number of faces, ϵ is the *Euler characteristic*, and X is the "adjustment" parameter easily determined by rules 1–7 of ref 1a. In terms of molecular orbital theory, the parameter X is best interpreted as the number of "missing" antibonding cluster orbitals.[4] Note that eq 1a applies to 1-, 2-, and 3-D systems (for 1- and 2-D clusters, X is normally zero). Equation 1b applies to 2- and 3-D clusters since, for these systems, the number of edges is given by the Euler relation $E = V + F - \epsilon$, where $\epsilon = 1$ and 2 for 2- and 3-D systems, respectively.

Topological vs. Skeletal Electron Pairs

The topological electron counting scheme assumes that each vertex atom contributes three orbitals to cluster bonding. This is a reasonable assumption since it has been used successfully in the SEP theory[5] and in isolobal analogy.[6,7] (Note that this assumption is almost always true for main-group elements but may or may not be true for transition metals since the latter have more orbitals available for bonding.[8]) If B is the number of *bonding* orbitals formed by the $3V$ skeletal orbitals for a given polyhedron with V vertices where $V = V_n + V_m$, then the total number of topological electron pairs is given by[4]

$$T = V_n + 6V_m + B \tag{2}$$

since the V_n s orbitals from the main-group elements and $6V_m$ (five d and one s) orbitals from the transition metals can be considered as "filled" (by electrons donated by the ligands or by valence electrons contributed by the vertex atoms). The parameter B can be interpreted as the number of *cluster bonding orbitals*. In terms of electrons filling these orbitals, B is the number of *skeletal electron pairs*, in the same context as the SEP theory.[5]

Equation 2 in effect separates the total number of electron pairs into two parts: viz., those occupying the energeticaly low-lying valence orbitals (V_n s orbitals for main-group elements, $5V_m$ d orbitals and V_m s orbitals for transition metals) and those (B) primarily responsible for "holding the cluster together". Such a partition, admittedly a crude approximation, is not without theoretical justification. For example, Lauher[8] first pointed out that the EHMO energy diagram of bare metal clusters (which were used as an approximation to metal cluster compounds) can be separated into two sets: a low-lying set of cluster valence molecular orbitals (CVMO) and a high-lying set of antibonding orbitals (HLAO). The empirical upper limit for the CVMOs was set by Lauher at the atomic p level of the isolated metal atoms. The total number of cluster valence electrons, N (or CVE in Lauher's terminology), can then be predicted by filling all the CVMOs. Ciani and Sironi[9] extended Lauher's idea and performed independent EHMO calculations on larger cluster systems and found that "any *compact closed-packed* cluster compound should have $6M + 7$ CVMOs or a number very close to this" (where M is the *total number* of metal atoms). As pointed out by Ciani and Sironi,[9] the factor $6M$ can be interpreted as originating from the fact that, for a large cluster, each metal contributes a maximum of six orbitals (five d and one s valence orbitals), as is the case in bulk metals. They also interpreted the near constancy of B' ($B' \approx 7$) for "closed-packed" polyhedra as due to the fact that "on adding atoms to a cluster each formally contributes 6 more CVMOs to the total number" (vide infra).

The important feature in eq 2 is that we have extended Ciani and Sironi's $6M + 7$ rule to include *non-close-packed* clusters and clusters containing main-group elements and/or transition metals. A more recent Fenske–Hall approximate molecular orbital calculation[10] on trinuclear metal clusters also suggested that, to a first approximation, each metal atom contributes three orbitals, predominantly of p character, to the metal–metal interaction.

Combining eq 1b and 2 yields

$$B = 3V - E + X \tag{3a}$$

$$= 2V - F + \epsilon + X \tag{3b}$$

---

(1) (a) Teo, B. K. *Inorg. Chem.* **1984**, *23*, 1251. (b) Teo, B. K.; Longoni, G.; Chung, F. R. K. *Inorg. Chem.* **1984**, *23*, 1257.

(2) Mingos, D. M. P. *Inorg. Chem.* **1985**, *24*, 114.

(3) Teo, B. K. *Inorg. Chem.* **1985**, *24*, 115.

(4) Teo, B. K. *Inorg. Chem.* **1985**, *24*, 1627.

(5) (a) Williams, R. E. *Inorg. Chem.* **1971**, *10*, 210. (b) Rudolph, R.; Pretzer, W. R. *Inorg. Chem.* **1972**, *11*, 1974. (c) Wade, K. *J. Chem. Soc. D* **1971**, 792; *Inorg. Nucl. Chem. Lett.* **1972**, *8*, 559, 563. (d) Wade, K. *Chem. Br.* **1975**, *11*, 177. (e) Wade, K. *Adv. Inorg. Chem. Radiochem.* **1976**, *18*, 1. (f) Mingos, D. M. P. *Nature (London), Phys. Sci.* **1972**, *236*, 99. (g) Mason, R.; Thomas, K. M.; Mingos, D. M. P. *J. Am. Chem. Soc.* **1973**, *95*, 3802. (h) Mingos, D. M. P. *J. Chem. Soc., Chem. Commun.* **1983**, 706. (i) Mingos, D. M. P. *J. Organomet. Chem.* **1983**, *251*, C13.

(6) (a) Elian, M.; Chen, M. M. L.; Mingos, D. M.; P.; Hoffmann, R. *Inorg. Chem.* **1976**, *15*, 1148. (b) Hoffmann, R. *Science (Washington, D.C.)* **1981**, *211*, 995. (c) Schilling, B. E. R.; Hoffmann, R. *J. Am. Chem. Soc.* **1979**, *102*, 3456. (d) Hoffmann, R.; Schilling, B. E. R.; Bau, R.; Kaesz, H. D.; Mingos, D. M. P. *J. Am. Chem. Soc.* **1978**, *100*, 6088.

(7) (a) Halpern, J. *Discuss. Faraday Soc.* **1968**, *46*, 7. (b) Ellis, J. E. *J. Chem. Educ.* **1976**, *53*, 2. (c) Stone, F. G. A. *Acc. Chem. Res.* **1981**, *14*, 318. (d) Mingos, D. M. P. *Trans. Am. Crystallogr. Assoc.* **1980**, *16*, 17. (e) Albright, T. A. *Trans. Am.* crystallogr. *Assoc.* **1980**, *16*, 35.

(8) (a) Lauher, J. W. *J. Am. Chem. Soc.* **1978**, *100*, 5305. (b) Lauher, J. W. *J. Am. Chem. Soc.* **1979**, *101*, 2604. (c) Lauher, J. W. *J. Organomet. Chem.* **1981**, *213*, 25.

(9) Ciani, G.; Sironi, A. *J. Organomet. Chem.* **1980**, *197*, 233.

(10) Kostic, N. M.; Fenske, R. F. *Inorg. Chem.* **1983**, *22*, 666.

0020-1669/85/1324-4209$01.50/0

Chart I. Cubic Clusters with Varying Numbers of Faces

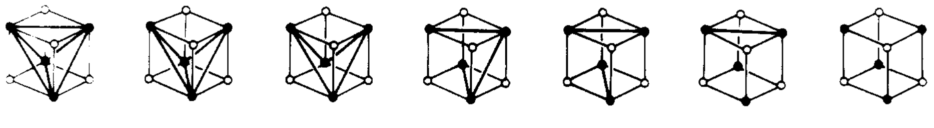

F =	12	11	10	9	8	7	6
B =	6	7	8	9	10	11	12
N =	68	70	72	74	76	78	80

For any given polyhedron, B can be readily calculated from V, F, and X. Equation 3 thus provides a bridge between the TEC and the SEP approaches. Note that *B depends only on the total number of vertices (V) and not on the relative abundance of non-metal (V_n) and transition metal (V_m) atoms.* With some exceptions, the B values predicted by TEC for *close-packed* clusters generally agree with that calculated by Ciani and Sironi.[9] Our results, however, show that B is *not* a constant for different types of polyhedra of varying degrees of nuclearity.

A comparison of our B values with those predicted by the SEP rule for deltahedral clusters ($B = V + 1$) revealed good agreement[4] in general except for the following deltahedra: For the trigonal bipyramid, triangular dodecahedron, tricapped trigonal prism, and bicapped square antiprism, the SEP theory agrees with one of the two B values predicted by our theory (see, however, a recent work by O'Neill and Wade[11]). For an octadecadeltahedron with 11 vertices, our method predicts $B = 11$ whereas the SEP rule predicts $B = 12$, which is observed in $B_{11}H_{11}^{2-}$. It is conceivable that a B value of 12 corresponds to a convex octadecadeltahedron. (Note that the 11-vertex octadecadeltahedron is not a convex polyhedron.)

The SEP theory applies not only to deltahedral clusters (excluding the tetrahedron and bicapped tetrahedron) but also to polyhedra that can be visualized as derivable from a deltahedron with 1, 2, or 3 missing vertices with $B = V + 2$, $V + 3$, or $V + 4$, respectively. These latter polyhedra are commonly called *nido* ("nestlike"), *arachno* ("weblike") and *hypho* ("netlike") polyhedra, respectively. This is sometimes termed as the *debor* principle.[5,12] Another concept in the SEP theory is the *capping*[13] principle,[12] which states that capping does not alter the number of skeletal electron pairs of the parent polyhedron. Generally speaking, the predictions by the TEC and the SEP approaches are similar (see, however, the section Ways TEC Differs from Other Approaches).

Encapsulation

Encapsulated (bulk) atoms are treated as electron contributors and not as part of the cluster framework in eq 1–3. For example, the icosahedron, bicapped pentagonal prism, cuboctahedron (ccp), and twinned cuboctahedron (hcp) are considered as 12-vertex polyhedra rather than 13-metal clusters (since each can have an encapsulated atom). In the comparison of our results with those of Lauher[8] or Ciani and Sironi,[9] care must be taken to avoid the confusion of *number of vertices*, V, and the *total number of metal atoms*, M. For example, an icosahedron of metal atoms, having $V = 12$ and $B = 13$, requires a total of $T = 6V + B = 85$ electron pairs whereas the same icosahedron with an encapsulated metal atom (a 13-atom cluster) having $M = 13$ and $B' = 7$ also requires $T = 6M + B' = 85$ electron pairs. Obviously, when the icosahedral cavity is filled with a metal atom, the B value is decreased from 13 to the "close-packed" value of 7. In fact, for *close-packed* high-nuclearity *metal* clusters, B' corresponds to the B value of the encapsulated unit: e.g., $B' = 7, 5, 6, 6, 7$ for the complete encapsulation of an atom, a dimer, a triangle, a tetrahedron, and an octahedron, respectively (cf. eq 3).

For a given nuclearity (V), as the number of faces (F) decreases, the value of B increases, parallel to the increase in the cage size. Generally speaking, a larger B value implies a larger cavity, which can incorporate a larger atom (or more atoms). For example $B \geq 7$ for the encapsulation of C or N atoms, $B \geqslant 11$ for S or P, and $B \geqslant 13$ for larger atoms such as Sb or metal atoms. For the C–C moiety, $B \geqslant 10$.

Incomplete encapsulation can occur if the cavity or the B value is not large enough. For example, for $V = 5$ and 6, the maximum B values are 8 and 9, respectively, not enough to completely encapsulate a phosphorus or a sulfur atom. This may be one of the reasons that the pentametal cluster $Ru_5(CO)_{16}(\mu\text{-}PPh_2)(\mu_5\text{-}P)$[14] and the hexametal cluster $[Co_6(CO)_{14}(\mu\text{-}CO)_2(\mu_6\text{-}P)]^-$[15] adopt somewhat open structures with *semiinterstitial* phosphorus atoms.

Counting Electrons

For the sake of convenience, we consider each atom or ligand, regardless of its formal oxidation state, a neutral entity. This often alleviates the difficult task of assigning charges to individual atoms or group of atoms. For example, each nickel atom in the cube-like $Ni_8(\mu_4\text{-}PPh)_6(CO)_8$[16] cluster will have 10 electrons, each of the quadruply bridging PPh groups will donate 4 electrons to the cluster (note that each phosphorus atom uses 1 of its 5 valence electrons to form a covalent bond with the phenyl ring), and each of the eight terminal carbonyls is a 2-electron donor. Similarly, each cobalt atom in the cuneane-like $Co_8(\mu_5\text{-}S)_2(\mu_4\text{-}N\text{-}t\text{-}Bu)_2(\mu_3\text{-}N\text{-}t\text{-}Bu)_2(NO)_8$[17] contributes 9 electrons, each pentagonally bridging sulfur donates 4 electrons, eacn N-*t*-Bu group donates 4 electrons, and each linear nitrosyl group donates 3 electrons to the cluster. It should be noted that a carbonyl ligand contributes 2 electrons, regardless of the mode of binding, provided that the oxygen atom is not involved. If the oxygen atom also binds to the cluster, then the electron count increases as is observed in $Fe_4(CO)_{13}H^-$,[18] where the bridging carbonyl group acts as a 4-electron rather than a 2-electron donor.

For a metal cluster with bridging ligands, eq 1 can be applied to either the metal core or the metal–(bridging ligand) cluster framework. For example, $Ni_8(\mu_4\text{-}PPh)_6(CO)_8$[16] can be considered as either a cube (Ni_8) or a hexacapped cube (Ni_8P_6). In the former case, $V_n = 0$, $V_m = 8$, $F = 6$, $X = 0$, eq 1b predicts $N = 120$ electrons, as is indeed observed ($N_{obsd} = 8 \times 10(Ni) + 6 \times 4(\mu_4\text{-}PR) + 8 \times 2(CO) = 120$). In the latter case, $V_n = 6$, $V_m = 8$, $F = 24$, $X = 6$ (capping six square faces), eq 1b predicts $N = 132$ electrons, which again agrees with the observed value of

---

[11] O'Neill, M. E.; Wade, K. *Polyhedron* **1984**, *3*, 199.

[12] The capping and debor princples can also be derived in the following manner. For a polyhedral cluster with V vertices, F faces, and an X value, the number of skeletal electron pairs B is given by eq 3b. If we cap one of the n-gonal faces, rule 2 predicts that the X value goes up by $(n - 3)$. At the same time, the number of vertices goes up by 1 and the number of faces increases by $(n - 1)$. The latter arises because n new faces are formed while the original n-gonal face (a face with n sides) has been covered by the capping atom. The number of skeletal electron pairs for the new polyhedron is then $B' = 2V' - F' + 2 + X' = 2(V + 1) - [F + (n - 1)] + 2 + [X + (n-3)] = 2V - F + 2 + X = B$. Hence the number of skeletal electron pairs remains unchanged upon capping, as first pointed out by Mingos.[13] The exact reversal of the above reasoning applies to the derivation of the *debor* principle.

[13] See ref 23 of: Evans, D. G.; Mingos, D. M. P. *Organometallics* **1983**, *2*, 435.

[14] MacLaughlin, S. A.; Taylor, N. J.; Carty, A. J. *Inorg. Chem.* **1983**, *22*, 1409.

[15] Chini, P.; Ciani, G.; Martinengo, S.; Sironi, A.; Longhetti, L.; Heaton, B. T. *J. Chem. Soc., Chem. Commun.* **1979**, 188.

[16] Lower, L. D.; Dahl, L. F. *J. Am. Chem. Soc.* **1976**, *98*, 5046.

[17] Chu, C. T. W. Ph.D. Thesis, University of Wisconsin—Madison, 1977.

[18] Manassero, M.; Sansoni, M.; Longoni, G. *J. Chem. Soc., Chem. Commun.* **1976**, 919.

Chart II. Octavertex Clusters with Varying Numbers of Faces

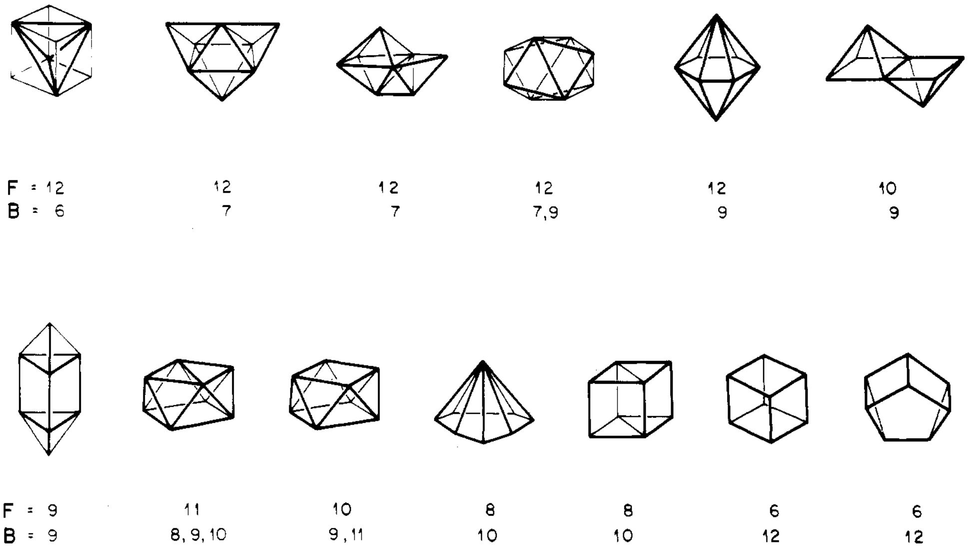

$N_{obsd} = 8 \times 10(Ni) + 6 \times 5(P) + 6 \times 1(Ph) + 8 \times 2(CO) = 132$.

Clusters with Varying Numbers of Vertices (V_m and V_n)

As is evident from eq 1, successive replacements of non-metal by metal vertices within a cluster causes the electron counts (N) to increase by 10/step. This can be illustrated by the series of tetrahedral clusters ($F = 6$ and $X = 0$): with V_n:V_m = 4:0, 3:1, 2:2, 1:3, and 0:4, eq 1b predicts N = 20, 30, 40, 50, and 60 electrons, as are indeed observed in, for example, $\mathbf{As_4}$, $\mathbf{Co}(CO)_3\mathbf{As_3}$,[19] $\mathbf{Co_2}(CO)_6\mathbf{As_2}$,[20] $\mathbf{Co_3}(CO)_9\mathbf{As}$,[21] and $\mathbf{Co_4}(CO)_{12}$,[22] respectively. (The cluster cores are boldfaced.) With $V = 4$, $F = 6$, and $X = 0$, eq 3 predicts $B = 6$.

Clusters with Varying Numbers of Faces (F)

For the same number of vertices, a cluster with less number of faces F will have a higher electron count N (cf. eq 1b) and a larger number of skeletal electron pairs B. This is understandable since the addition of electrons to a cluster with bonding edges generally causes some of the edges to rupture. That is, the added electrons populate the low-lying cluster antibonding orbitals. With less number of bonding edges, the number of faces decreases and the cluster adopts a more open structure. If the antibonding cluster orbitals are degenerate and partially occupied, the molecule may also undergo Jahn–Teller distortion to lower symmetry. A beautiful series of cube-like (or cubane-like) clusters is shown in Chart I. For these clusters, $X = 0$. Examples (N_{obsd}) include $\mathbf{Fe_4}(NO)_4\mathbf{S_4}$[23] (68e), $Cp_2\mathbf{Mo_2S_4Ni_2}(CO)_2$[24] (70e), $\mathbf{Co_4}(NO)_4(\mathbf{N}CMe_3)_4$[25] (72e), $[Cp_4\mathbf{Fe_4Te_4}]^{2+}$[26] (74e); $Cp_4\mathbf{Fe_4S_4}$[27] (76e), $[Cp_4\mathbf{Co_4Te_4}]^{2+}$[26] (78e), and $Cp_4\mathbf{Co_4S_4}$[28] (80e). (Cp is η^5-C_5H_5.) As the number of faces F decreases, the number of skeletal electron pairs B increases stepwise from 6 in the completely *bonding* tetrahedron to 12 in the completely *nonbonding* tetrahedron. As a result, the clusters undergo the following distortions: $T_d \rightarrow C_{2v} \rightarrow D_{2d}$ (compressed) $\rightarrow C_2 \rightarrow D_{2d}$ (elongated) $\rightarrow C_{2v} \rightarrow T_d$. (Note that other distortions are also possible.[29])

Chart II depicts some eight-vertex clusters with varying numbers of faces. Examples include the following: tetracapped tetrahedral $\mathbf{Fe_4}(NO)_4\mathbf{S_4}$[23] ($B = 6$); bicapped octahedral $[\mathbf{Os_8}(CO)_{22}]^{2-}$[30] ($B = 7$); fused octahedral–(trigonal-bipyramidal) $\mathbf{Cu_2Ru_6C}(CO)_{16}(NCCH_3)_2$[31] ($B = 7$); triangular-dodecahedral *closo*-$\mathbf{B_8}H_8^{2-}$, $\mathbf{Fe_4}(CO)_{11}(H\mathbf{CC}Et)_2$[32] ($B = 9$), $\mathbf{B_4}H_4\mathbf{Co_4}Cp_4$[33a] ($B = 8$), $\mathbf{B_4}H_4\mathbf{Ni_4}Cp_4$[33b] ($B = 10$); hexagonal bipyramid with $B = 9$; edge-sharing bis-square-pyramidal[33c] $\mathbf{Os_6}(CO)_{16}(\mathbf{C_2}Me_2)\mathbf{C}$ ($B = 9$); bicapped (Δ^2) trigonal-prismatic $\mathbf{Cu_2Rh_6C}(CO)_{15}(NCCH_3)_2$[33d] ($B = 9$); bicapped ($\square^2$) trigonal prism with B = 8, 9, 10; square-antiprismatic $[\mathbf{Co_8C}(CO)_{18}]^{2-}$[34] ($B = 9$) and $\mathbf{B_8}H_{14}$, $\mathbf{Bi_8}^{2+}$,[35] $[\mathbf{Ni_8C}(CO)_{16}]^{2-}$[36] ($B = 11$); heptagonal-pyramidal $(\eta^7$-$\mathbf{C_7}H_7)\mathbf{V}(CO)_3$[37] ($B = 10$); square-face-sharing bitrigonal-prismatic $[\mathbf{Co_6Ni_2C_2}(CO)_{16}]^{2-}$[38] ($B = 10$); cubane $\mathbf{C_8}H_8$[39] and $\mathbf{Ni_8}(\mathbf{P}Ph)_6(CO)_8$[16] ($B = 12$); cuneane $\mathbf{C_8}H_8$,[40] $\mathbf{Co_4S_2}(\mathbf{N}$-$t$-$Bu)_4(NO)_8$[17] ($B = 12$). Note that for a given degree of nuclearity, triangulated polyhedra generally have the lowest B values while the 3-connected

---

(19) Foust, A. S.; Foster, M. S.; Dahl. L. F. *J. Am. Chem. Soc.* **1969**, *91*, 5631.

(20) Foust, A. S.; Foster, M. S.; Dahl, L. F. *J. Am. Chem. Soc.* **1969**, *91*, 5633.

(21) Vizi-Orosz, A.; Galamb, V.; Palyi, G.; Marko, L. M.; Bor, G.; Natile, G. *J. Organomet. Chem.* **1976**, *107*, 235.

(22) Wei, C. H.; Dahl, L. F. *J. Am. Chem. Soc.* **1966**, *88*, 1821. Wei, C. H. *Inorg. Chem.* **1969**, *8*, 2384.

(23) Gall, R. S.; Chu, C. T. W.; Dahl, L. F. *J. Am. Chem. Soc.* **1974**, *96*, 4019.

(24) Curtis, M. D.; Williams, P. D. *Inorg. Chem.* **1983**, *22*, 2661.

(25) Gall, R. S.; Connelly, N. G.; Dahl, L. F. *J. Am. Chem. Soc.* **1974**, *96*, 4017.

(26) Szmanda, C. R. Ph.D. Thesis, University of Wisconsin—Madison, 1978.

(27) (a) Wei, C. H.; Wilkes, G. R.; Treichel, P. M.; Dahl, L. F. *Inorg. Chem.* **1966**, *5*, 900. (b) Schunn, R. A.; Fritchie, C. J., Jr.; Prewitt, C. T. *Inorg. Chem.* **1966**, *5*, 892. (c) Trinh, T.; Teo, B. K.; Ferguson, J. A.; Meyer, T. J.; Dahl, L. F. *J. Am. Chem. Soc.* **1977**, *99*, 408.

(28) Simon, G. L.; Dahl, L. F. *J. Am. Chem. Soc.* **1973**, *95*, 2164.

(29) Teo, B. K. Ph.D. Thesis, University of Wisconsin—Madison, 1973.

(30) Jackson, P. F.; Johnson, B. F. G.; Lewis, J.; Raithby, P. R. *J. Chem. Soc., Chem. Commun.* **1980**, 60.

(31) Bradley, J. S.; Pruett, R. L.; Hill, E.; Ausell, G. B.; Leonowicz, M. E.; Modrick, M. A. *Organometallics* **1982**, *1*, 74.

(32) Sappa, E.; Tiripicchio, A.; Camellini, M. T. *J. Chem. Soc., Dalton Trans.* **1978**, 419.

(33) (a) Pipal, J. R.; Grimes, R. N. *Inorg. Chem.* **1979**, *18*, 257. (b) Bowser, J. R.; Bonny, A.; Pipal, J. R.; Grimes, R. N. *J. Am. Chem. Soc.* **1979**, *101*, 6229. (c) Eady, C. R.; Fernandez, J. M.; Johnson, B. F. G.; Lewis, J.; Raithby, P. R.; Sheldrick, G. M. *J. Chem. Soc., Chem. Commun.* **1978**, 421. (d) Albano, V. G.; Braga, D.; Martinengo, S.; Chini, P.; Sansoni, M.; Strumolo, D. *J. Chem. Soc., Dalton Trans.* **1980**, 52.

(34) Albano, V. G.; Chini, P.; Ciani, G.; Martinengo, S.; Sansoni, M. *J. Chem. Soc., Dalton Trans.* **1978**, 463.

(35) Krebs, B.; Hucke, M.; Brendel, C. S. *Angew. Chem., Int. Ed. Engl.* **1982**, *21*, 445.

(36) Longoni, G.; Ceriotti, A.; Della Pergola, R.; Manassero, M.; Perego, M.; Piro, G.; Sansoni, M. *Philos. Trans R. Soc. London A* **1982**, *308*, 47.

(37) Allegra, G.; Perego, G. *Ric. Sci., Part 2: Sez. A* **1961**, *1*, 362; *Chem. Abstr.* **1965**, *62*, 4724.

(38) Longoni, G.; Ceriotti, A.; Della Pergola, R.; Manassero, M.; Sansoni, M., private communication.

(39) (a) Eaton, P. E.; Cole, T. W. *J. Am. Chem. Soc.* **1964**, *86*, 3157. (b) Barborak, J. C.; Watts, L.; Pettit, R. *J. Am. Chem. Soc.* **1966**, *88*, 1328. (c) Chin, C. G.; Cuts, H. W.; Masamune, S. *Chem. Commun.* **1966**, 880. (d) Barborak, J. C.; Watts, L.; Pettit, R. *J. Am. Chem. Soc.* **1966**, *88*, 1328.

(40) (a) Cassar, L.; Eaton, P. E.; Halpern, J. *J. Am. Chem. Soc.* **1970**, *92*, 6366. (b) Criegee, R.; Askani, R. *Angew. Chem., Int. Ed. Engl.* **1968**, *7*, 537.

polyhedra have the highest B values.

Ways TEC Differs from Other Approaches

The ways in which the TEC approach differs from other electron counting rules may be summarized as follows.

Multiple Electron Counts. Multiple X values imply multiple electron counts. The observed count(s) generally falls (fall) within the range of predicted values. Multiple electron counts can happen in several different ways. The obvious one is the multiple X values in the basic TEC rules. For example, TEC predicts $X = 0, 2$ for trigonal-bipyramidal clusters, giving rise to $B = 6, 8$, respectively (via eq 2). The majority of clusters adopt $B = 6$, as exemplified by $[\mathbf{FeCoP_3}LL']^{2+}$,[41] where L = 1,1,1-tris((diphenylphosphino)methyl)ethane and L′ = 1,1,1-tris((diethylphosphino)methyl)ethane. A few, however, have $B = 8$, as observed in $[\mathbf{Pd_2P_3}L_2]^{+}$[42] and $[\mathbf{Ni_5}(CO)_{12}]^{2-}$.[43] Yet fewer examples can be found for $6 < B < 8$, as in the capped-trigonal-prismatic $Cp_3\mathbf{Ni_3Os_3}(CO)_9$[44] with $B = 7.5$. Another example is the square antiprism where the TEC approach predicts $B = 9, 11$ for $X = 1,3$, respectively. The majority of square-antiprismatic clusters adopt $B = 11$, as exemplified by $\mathbf{Bi_8}^{2+}$[45] and $[\mathbf{Ni_8}C(CO)_{16}]^{2-}$.[46] A few, however, adopt $B = 9$, as found in $[\mathbf{Co_8}C(CO)_{18}]^{2-}$.[47] (Note that trigonal bipyramids with $B = 8$ and square antiprisms with $B = 9$ follow neither EAN nor SEP rules.) The reasons for such multiple electron counts have been discussed in ref 1 and 4.

A second type of multiple electron counts occurs when there are alternate routes to a given polyhedron. This can occur when the cluster geometry can be built from lower nuclearity clusters with multiple electron counts and/or when it can be obtained by slight deformation of another polyhedron with multiple electron counts. For example, as shown in Chart XIb of ref 4, the bicapped (C_{2v}) trigonal prism can be obtained either by capping two square faces of a trigonal prism, giving rise to $X = 2$ via rule 2 and $B = 9$ (eq 3), or by removing 2 electrons from one square face of a square antiprism to give two trigonal faces, resulting in $X = 1, 3$ via rule 7 and $B = 8, 10$ (eq 3). The observed B value in B_8H_{12} is 10.

Note that where multiple electron counts arise for a given structure, the SEP approach usually agrees with the higher electron counts predicted by the TEC method (except for the trigonal bipyramid and octahedron, where the reverse is true).[3] In some cases, the SEP rule may also give rise to more than one electron count. For example, a capped (□) trigonal prism may be regarded as an *arachno*-tricapped trigonal prism, giving rise to $B = 10$ (via the original SEP rule) or a capped trigonal prism, resulting in $B = 9$ (via the extended SEP rule). The observed B value in $\mathbf{Fe_4}(CO)_{11}(NEt)(ONEt)$[48] is 9, as is predicted by the TEC approach ($B = 2 \times 7 - 8 + 2 + 1 = 9$).

Fused and Higher Polyhedral Clusters. Rule 6 of TEC is useful in determining the X value for vertex-, edge-, and face-sharing polyhedra. We shall discuss some of these examples.

The vertex-sharing bitetrahedron has an X value of 1 since each tetrahedron contributes $X = 0$ and sharing a common vertex increases X by 1. With 7 vertices and 8 faces, eq 3 predicts a B value of 9, as is indeed observed in $\mathbf{Os_5}S_2(CO)_{14}H_2$.[49] For the edge-sharing bis(square pyramid) shown in Chart II, $B = 9$ can be readily calculated from eq 2 with $V = 8$, $F = 10$, and $X = 1$. This agrees with the same value observed in $\mathbf{Os_6}(CO)_{16}(C_2Me_2)C$.[50]

The majority of the fused polyhedra are face-sharing. Rule 6 predicts $X = 0$ for face-sharing, regardless of the type (trigonal, tetragonal, etc.) of the face shared. The total X value for the fused polyhedron is thus the simple sum of the X values of its components. (The only exception is that the overall X value decreases by the number of hidden edges (bonds), if any; vide infra.) For example, the fused octahedron and trigonal bipyramid (cf. Chart II) is observed in $\mathbf{Ru_6}C(CO)_{16}\mathbf{Cu_2}(NCCH_3)_2$[31] with $B = 7$, as predicted.

The face-sharing bis(square antiprism) structure is predicted to have $X = 2, 4, 6$, giving rise to $B = 10, 12, 14$ via eq 2 (note that each square antiprism has $X = 1, 3$ and $B = 9, 11$), in excellent agreement with the observed B values of 11-12 in $[\mathbf{Rh_{12}}C_2(CO)_{24}]^{n-}$ (n = 2-4).[51] This example illustrates that multiple X values usually mean that multiple electron counts are energetically accessible and that the observed electron counts often fall within the predicted range.

The face-to-face fused trioctahedral cluster $[\mathbf{Rh_{11}}(CO)_{23}]^{3-}$[52] can conceptually be thought of being formed by fusing *three* octahedra, sharing three adjacent faces (cf. Chart XII of ref 1b). As a result, there is one hidden edge completely embedded within the cluster. Hence $X = 3 \times 1$ (octahedron) $- 1$ (hidden edge) $= 2$. With $V = 11$ and $F = 18$, $B = 8$ is predicted, as is indeed observed. We predict that addition of 2 electrons to $[\mathbf{Rh_{11}}(CO)_{23}]^{3-}$ should produce a similar structure without the hidden edge (central bond).

The anionic cluster $[\mathbf{Ni_{12}}(CO)_{21}H_{4-n}]^{n-}$ (n = 2, 3, 4)[53] has a hexagonal close-packed (A, B, A pattern) structure without the encapsulated metal atom (note that the layer pattern of Chart XV of ref 1b was incorrectly labeled). The observed B value of 11 agrees with one of the two predicted values (8 or 11).

The strength of the TEC approach lies in its application to complicated fused or connected polyhedral clusters of high nuclearity. While the extension[5h,i] of the SEP rule to some of these clusters has been suggested, it requires different equations for different ways of condensation. Furthermore, its applications to, for example, the three latter clusters discussed above are not obvious.

"Electron-Rich" and "Electron-Deficient" Clusters

It is important to note that the success of any electron counting scheme depends largely on the energy gap between the highest occupied molecular orbital (HOMO) and the lowest unoccupied molecular orbital (LUMO) of a given cluster. As the nuclearity of the cluster increases, the molecular orbital energy level spacings decrease rapidly. At some point, the HOMO–LUMO gap may become small enough such that it is possible to populate the energetically low-lying LUMOs, giving rise to higher electron counts, or to depopulate the energetically high-lying HOMOs, resulting in lower electron counts. Depending upon the character of the orbital(s) involved, as well as the symmetry and the energetics of the system, this may or may not affect the cluster framework. Here we consider three examples of "electron-rich" and one example of "electron-deficient" clusters.

The tetracapped (□^{2}, ⬠^{2}) pentagonal-prismatic structure (cf. Chart XXIII of ref 1b) has been observed in the pentadecametal cluster $[\mathbf{Rh_{15}}C_2(CO)_{28}]^{-}$.[54] The X value is 6 since each square cap and each pentagonal cap contribute an X value of 1 and 2, respectively (cf. rule 2). With 14 vertices and 21 faces, eq 2 predicts a B value of 15. The observed value in the pentadecarhodium cluster is 16. The extra electron pair is believed to have

---

(41) Bianchini, C.; DiVaira, M.; Meli, A.; Sacconi, L. *Inorg. Chem.* **1981**, *20*, 1169.

(42) Dapporto, P.; Sacconi, L.; Stoppioni, P.; Zanobini, F. *Inorg. Chem.* **1981**, *20*, 3834.

(43) Longoni, G.; Chini, P.; Lower, L. D.; Dahl, L. F. *J. Am. Chem. Soc.* **1975**, *97*, 5034.

(44) Sappa, E.; Lanfranchi, M.; Tiripicchio, A.; Camellini, M. T. *J. Chem. Soc., Chem. Commun.* **1981**, 995.

(45) Krebs, B.; Hucke, M.; Brendel, C. S. *Angew. Chem., Int. Ed. Engl.* **1982**, 21, 445.

(46) Longoni, G.; Ceriotti, A.; Della Pergola, R.; Manassero, M.; Perego, M.; Piro, G.; Sansoni, M. *Philos. Trans. R. Soc. London, A* **1982**, *308*, 47.

(47) Albano, V. G.; Chini, P.; Ciani, G.; Martinengo, S.; Sansoni, M. *J. Chem. Soc., Dalton Trans* **1978**, 463.

(48) Gervasio, G.; Rossetti, R.; Stanghellini, P. L. *J. Chem. Soc., Chem. Commun.* **1977**, 387.

(49) Adams, R. D.; Horvath, I. T. *Organometallics* **1983**, *2*, 1257.

(50) Eady, C. R.; Fernandez, J. M.; Johnson, B. F. G.; Lewis, J.; Raithby, P. R.; Sheldrick, G. M. *J. Chem. Soc., Chem. Commun.* **1978**, 421.

(51) Martinengo, S., private communication.

(52) Fumagalli, A.; Martinengo, S.; Ciani, G.; Sironi, A. *J. Chem. Soc., Chem. Commun.* **1983**, 453.

(53) Broach, R. W.; Dahl, L. F.; Longoni, G.; Chini, P.; Schultz, A. J.; Williams, J. M. *Adv. Chem. Ser.* **1978**, *No. 167*, 93.

(54) Albano, V. G.; Sansoni, M.; Chini, P.; Martinengo, S.; Strumolo, D. *J. Chem. Soc., Dalton Trans* **1976**, 970.

caused the lengthening of two Rh–Rh distances from the average value of 2.87 Å to 3.33 Å. Another example is the hexacapped trigonal-antiprismatic cluster[55] (Chart XIV of ref 1b) $[\mathbf{Fe_6Pd_6}(CO)_{24}H]^{3-}$, which is predicted to have $B = 7$. The observed value is 8. The extra electron pair may be the cause of the long Pd–Pd distance of 2.88 (av) Å though it may also be due to the hydride in the trigonal-antiprismatic Pd_6 cage (proposed site). For the corner-sharing dicube $X = 1$ since each cube has $X = 0$. The B value is predicted to be 21, which is two electron pairs less than that of 23 observed in $Me_6\mathbf{Zn_7O_8}Me_8$.[56] The extra electron pairs may enter the antibonding Zn–O orbital framework.

The $[Pt_6(CO)_{12}]^{2-}$ dianion,[57] which has a slipped trigonal-prismatic structure, has a B value of 7 instead of the predicted value of 9. This may be due to the depopulation of the highest occupied e′ orbitals for a regular trigonal prism. It should be emphasized, however, that the electron deficiency in Pt clusters is probably related to its tendency to adopt a 16- rather than an 18-electronic configuration.

Conclusion

In summary, we have shown in this paper that the topological electron counting (TEC) theory developed recently by us[1] can be extended to include clusters containing both non-metal and metal atoms as well as clusters of lower dimensions (1- or 2-D).

A comparison is made, and a bridge established, between the skeletal electron pair (SEP) and the TEC theories, thereby providing an alternative (and sometimes complementary) way of calculating the number of skeletal electron pairs.

The correlation between the *cage* size and the number of *skeletal electron pairs* (B) is discussed. It is evident that larger encapsulated atoms require a larger B value and incomplete encapsulation can occur if B is not large enough. The difference between $T = 6V + B$ and $T = 6M + B'$ in calculating the number of topological electron pairs of close-packed high-nuclearity metal clusters is emphasized.

It is shown that, for a given structure, successive replacement of main-group elements by transition metals as vertices increases the topological electron counts (N) by 10 without affecting the number of skeletal electron pairs (B). It is also illustrated that as the number of faces of a cluster decreases, the electron count increases and vice versa.

Ways in which the TEC approach differs from other electron counting schemes (multiple electron counts, application to fused or connected polyhedra) are illustrated by examples. Reasons for "electron-rich" and "electron-deficient" clusters are also discussed.

Acknowledgment. The author is grateful to Dr. G. Longoni for numerous discussions. Special thanks go to Prof. L. F. Dahl, Prof. J. Lauher, and Prof. D. M. P. Mingos for many helpful comments.

---

(55) Longoni, G.; Manassero, M.; Sansoni, M. *J. Am. Chem. Soc.* **1980**, *102*, 3242.

(56) Ziegler, M. L.; Weiss, J. *Angew. Chem., Int. Ed. Engl.* **1970**, *9*, 905.

(57) Calabrese, J. C.; Dahl, L. F.; Chini, P.; Longoni, G.; Martinengo, S. *J. Am. Chem. Soc.* **1974**, *96*, 2614.

Contribution from the Department of Chemistry,
University of Toledo, Toledo, Ohio 43606

Bridge-Cleavage Reactions of $[Pt_2Cl_2(\mu\text{-}Cl)_2(PCy_3)_2]$ (Cy = Cyclohexyl) with Dimethyl Sulfoxide and Dibenzyl Sulfoxide. Conversion of Trans-S-Bonded and Trans-O-Bonded Sulfoxide Complexes to the Cis-S-Bonded Isomers

J. A. Davies* and A. Sood

Received March 19, 1985

The synthesis of the dimeric halide-bridged platinum(II) complex $[Pt_2Cl_2(\mu\text{-}Cl)_2(PCy_3)_2]$ from the reaction of $[K][PtCl_3(C_2H_4)]$ with PCy_3 under high-dilution conditions was reported in 1981.[1] This precursor allowed entry into the series of complexes *trans*-$[PtCl_2(PCy_3)(L)]$ (L = CO, CN-*t*-Bu, NC_5H_5, SMe_2, $AsPh_3$, tertiary phosphine; *t*-Bu = *tert*-butyl, Me = methyl, Ph = phenyl) via bridge cleavage with the appropriate nucleophile, L.[1] In all cleavage reactions, the trans isomer of the mixed-ligand complex is quantitatively produced and only in the case where L = CO could the cis isomer be generated (in trace amounts) by catalytic isomerization with free CO.[1] The exceptional stability of these complexes with respect to thermal trans → cis isomerization is demonstrated by a complete lack of isomerization upon heating solutions of *trans*-$[PtCl_2(PCy_3)(L)]$ (L = SMe_2, NC_5H_5) in the presence of a 10-fold excess of L at 55 °C for 2 h.[1]

As part of an electrochemical study[2-5] of geometric and ligand effects on the redox chemistry of platinum(II) complexes we have recently prepared[5,6] a series of mixed-ligand complexes, $[PtCl_2(PPh_3)(L)]$ (L = thioether, sulfur-bonded sulfoxide), via bridge cleavage of $[Pt_2Cl_2(\mu\text{-}Cl)_2(PPh_3)_2]$. In one case we were able to isolate separately both cis and trans isomers where L = thioether (Bz_2S (Bz = benzyl)) but in all cases where L = sulfur-bonded sulfoxide we were able to isolate only the cis isomers. The stability of the trans isomers of $[PtCl_2(PCy_3)(L)]$ with respect to isomerization led us to investigate further the cleavage reactions of $[Pt_2Cl_2(\mu\text{-}Cl)_2(PCy_3)_2]$ with sulfur-containing nucleophiles.

Experimental Section

$[Pt_2Cl_2(\mu\text{-}Cl)_2(PCy_3)_2]$ was prepared by the literature method.[1] ^1H and $^{31}P\{^1H\}$ NMR spectra were recorded at 89.56 MHz (^1H) and 36.2 MHz (^{31}P) on a JEOL FX90Q spectrometer operating in the Fourier transform mode. Chemical shifts are referenced to internal tetramethylsilane (^1H) and external 85% phosphoric acid (^{31}P) with more positive values of the chemical shift representing deshielding. Infrared spectra were obtained for solid solutions in KBr on a Nicolet 5DX Fourier transform IR spectrometer..

Cleavage reactions were performed by adding a stoichiometric amount of the nucleophile to a dichloromethane solution of the dimer (ca. 25 mg) and refluxing overnight. The solids were precipitated with hexane and dried in air. The ^1H and $^{31}P\{^1H\}$NMR spectra were recorded for the $CDCl_3$ solutions of these solids as a function of time. After each reaction was >85% complete, as estimated by peak heights in the $^{31}P\{^1H\}$ NMR spectra, the solvents were removed in vacuo and the products washed with hexane and dried for IR analysis.

Results and Discussion

It is reported[1] that $[Pt_2(\mu\text{-}Cl)_2Cl_2(PCy_3)_2]$ is cleaved by SMe_2 to yield *trans*-$[PtCl_2(PCy_3)(SMe_2)]$, which resists isomerization at 55 °C for 2 h in the presence of excess SMe_2. The corresponding cleavage with Me_2SO forms a single new species observable in the $^{31}P\{^1H\}$ NMR spectrum with $\delta = 19.35$ and $^1J(^{195}Pt,^{31}P) = 3174$ Hz. The magnitude of the coupling constant is consistent with coordination of Me_2SO trans to PCy_3. The ^1H NMR spectrum shows that the methyl protons are substantially deshielded ($\delta = 3.20$; cf. $\delta = 2.49$ for Me_2SO itself) and coupled to platinum, $^3J(^{195}Pt,^1H) = 13$ Hz, as anticipated for an S-bonded sulfoxide.[7] The methyl proton resonance is considerably broadened, with a peak width at half-height of ca. 3.5 Hz, which we attribute to unresolved trans coupling, $^4J(^{31}P,^1H)$ (vide infra). When the compound is allowed to stand in $CDCl_3$ solution, in the presence of a trace amount of free Me_2SO, a very slow trans → cis isomerization occurs.[8] The $^{31}P\{^1H\}$ NMR spectrum shows a new species, with $\delta = 27.58$ and $^1J(^{195}Pt,^{31}P) = 3378$ Hz, appearing as resonances due to the trans isomer diminish in in-

---

(1) Anderson, G. K.; Clark, H. C.; Davies, J. A. *Inorg. Chem.* **1981**, *20*, 944.

(2) Davies, J. A.; Uma, V. *Inorg. Chim. Acta* **1983**, *76*, L305.

(3) Davies, J. A.; Uma, V. *J. Electroanal. Chem.* **1983**, *158*, 13.

(4) Davies, J. A.; Uma, V. *J. Electroanal. Chem.* **1984**, *179*, 273.

(5) Davies, J. A.; Hasselkus, C. S.; Scimar, C. N.; Sood, A.; Uma, V. *J. Chem. Soc., Dalton Trans.* **1985**, 209.

(6) Davies, J. A.; Jones, R. A.; Sood, A.; Uma, V.; Wright, T. C., to be submitted for publication.

(7) Davies, J. A. *Adv. Inorg. Chem. Radiochem.* **1981**, *24*, 115.

(8) Reaction of $[Pt_2Cl_2(\mu\text{-}Cl)_2L_2]$ (L = Me_2SO, Et_2SO) with L yields *trans*-$[PtCl_2L_2]$, which undergoes trans → cis isomerization via an associative mechanism: Annibale, G.; Bonivento, M.; Canovese, L.; Cattalini, L.; Michelon, G.; Tobe, M. L. *Inorg. Chem.* **1985**, *24*, 797.

0020-1669/85/1324-4213$01.50/0